

# Strain-tunable band gap in graphene/h-BN hetero-bilayer

Harihar Behera\* and Gautam Mukhopadhyay†

*Department of Physics, Indian Institute of Technology, Powai, Mumbai-400076, India*

## Abstract

Using full-potential density functional calculations within local density approximation (LDA), we predict that mechanically tunable band-gap and quasi-particle-effective-mass are realizable in graphene/hexagonal-BN hetero-bilayer (C/h-BN HBL) by application of in-plane homogeneous biaxial strain. While providing one of the possible reasons for the experimentally observed gap-less pristine-graphene-like electronic properties of C/h-BN HBL, which theoretically has a narrow band-gap, we suggest a schematic experiment for verification of our results which may find applications in nano-electromechanical systems (NEMS), nano opto-mechanical systems (NOMS) and other nano-devices based on C/h-BN HBL.

Keywords : *Nanostructures, Ab initio calculations, Electronic structure, Transport properties*

---

\*E-mail: harihar@phy.iitb.ac.in; harihar@iopb.res.in

†Corresponding author's E-mail: gmukh@phy.iitb.ac.in; g.mukhopa@gmail.com

# 1 Introduction

Recent experiments [1, 2] at Columbia University showing the successful fabrication of hexagonal BN (h-BN) gated graphene field effect transistors (BN-GFETs), consisting of both mono-layer graphene (MLG) and bilayer graphene (BLG) on h-BN gate/substrate which could be made arbitrarily thin (down to a mono-layer of h-BN), are among the important developments in the physics and material science of graphene [3, 4, 5, 6]. Graphene supported on h-BN exhibits superior electrical properties with performance levels comparable to those observed in suspended samples [1, 2, 6, 7]. On the other side, in the context of strain engineering of electronic properties of graphene, another significant experimental development [8] utilizes piezoelectric actuators to apply tunable biaxial compressive as well as tensile stresses to graphene on h-BN substrate, which allows a detailed study of the interplay between the graphene geometrical structures and its electronic properties. In this scenario, it is useful and interesting to explore the effect of biaxial strain on the band gap, Fermi-velocity and the quasi-particle-effective-mass of a graphene/h-BN hetero-bilayer (representing the smallest and the simplest form of BN-GFET), which is not only feasible but also desirable, since strain-engineering [9] of Si, SiGe, Ge has been successfully used in the semiconductor industry to impressively improve the performance levels of conventional metal-oxide-semiconductor field-effect transistors (MOSFETs), and recently [10] strain is seen as a solution for higher carrier mobility in nano MOSFETs.

In this paper, we theoretically explore the effect of symmetry preserving homogeneous in-plane biaxial strain (which mimics an experi-

mental condition [8] in which a flexible substrate supported graphene can be strained in a controllable way by piezoelectric actuators) on a hetero-bilayer (C/h-BN HBL) consisting of an MLG (C) and a mono-layer of h-BN, which is the smallest and simplest form of BN-GFET. Previous theoretical studies on graphene on h-BN substrate [11] and C/h-BN HBL [12, 13] reported the opening of a small energy band gap in graphene which varies with (a) the stacking order, (b) the separation distance of graphene from the h-BN, and (c) the externally applied perpendicular electric field. Other graphene/h-BN heterostructures such as MLG [14] and BLG [15] sandwiched between two mono-layers of h-BN have also been theoretically shown to have (external) electric-field-tunable electronic properties. However, a detailed study of strain-engineered band gap of C/h-BN HBL is not available, although the effects of various strain distributions on mono-layer h-BN [16] and graphene [17, 18, 19, 20] have been reported recently. Theoretically it is shown that the high band gap of mono-layer h-BN is strain-tunable [16], the gap-less nature of graphene is robust against small and moderate deformations [17, 18, 19, 20]. On the experimental side, Raman spectroscopy studies [8, 21, 22, 23, 24] of graphene reveal that both biaxial [8] and uni-axial [21, 22, 23, 24] strains affect the Raman Peaks; the transport properties of strained graphene have been investigated by depositing samples on stretchable substrates [25]. Insights from these studies suggest a detectable strain-controlled band-gap in a composite structure like C/h-BN HBL. This expectation has, in fact, been borne out by the results of our present study. It is shown that the ground state direct band gap ( $\simeq 59$  meV) of C/h-BN HBL increases with biaxial tensile strain and decreases with compressive strain, whereas the Fermi ve-

licity of charge carriers follows a reverse trend. Moreover, the variation of computed average effective masses ( $m^*$ ) of charge carriers (electrons or holes) with strain is more pronounced with increasing trend for tensile strain and decreasing trend for compressive strain. These should affect the carrier mobility, conductivity and optical properties of C/h-BN HBL which may be verified experimentally for which we propose schematically a realistic experimental set-up.

## 2 Computational Methods

Our first-principles study of electronic structure of C/h-BN HBL is based on full-potential (linearized) augmented plane wave plus local orbital (FP-(L)APW+lo) method[26], which is a descendant of FP-LAPW method[27]. We use the elk-code[28] and the Perdew-Zunger variant of LDA[29], the accuracy of which has been successfully tested in our previous work [30] on graphene and silicene (silicon analog of graphene). The plane wave cut-off of  $|\mathbf{G} + \mathbf{k}|_{max} = 8.0/R_{mt}$  (a.u.<sup>-1</sup>) ( $R_{mt}$  = the smallest muffin-tin radius) was chosen for plane wave expansion in the interstitial region. The Monkhorst-Pack [31]  $k$ -point grid of  $20 \times 20 \times 1$  is used for structural optimization and of  $30 \times 30 \times 1$  for electronic calculations of C/h-BN BLG with simulated homogeneous in-plane biaxial strains up to  $\pm 15\%$ . Our consideration of strains up to 15% is motivated by recent theoretical calculations [32 – 34] as well as experiments [35] which demonstrated that graphene can sustain in-plane tensile elastic strain in excess of 20%; Kim et al. [25] have measured resistances of graphene films transferred to pre-strained and unstrained PDMS substrates with respect to uni-axial tensile strain ranging from 0% to 30%. Although in-plane homoge-

neous biaxial strains up to  $\pm 15\%$  have been considered theoretically in [36], the maximum compressive strain graphene can sustain is unclear to us. However, for the sake of symmetry and as a matter of curiosity, we have considered strains up to  $-15\%$ . The total energy was converged within  $2\mu\text{eV}/\text{atom}$ . We simulate the 2D-hexagonal structure of C/h-BN BLG as a 3D-hexagonal super-cell with a large value of  $c$ -parameter ( $c = 40$  a.u.) by considering the primitive vectors of the unit cell as

$$\mathbf{a} = (1/2) a \mathbf{e}_x - (\sqrt{3}/2) a \mathbf{e}_y \quad (1)$$

$$\mathbf{b} = (1/2) a \mathbf{e}_x + (\sqrt{3}/2) a \mathbf{e}_y \quad (2)$$

$$\mathbf{c} = c \mathbf{e}_z \quad (3)$$

where  $a$  is the in-plane lattice parameter and other symbols have their usual meanings. The value of  $a$  was varied to simulate the application of homogeneous in-plane biaxial stress (since  $|\mathbf{a}| = |\mathbf{b}| = a$ ) to C/h-BN HBL. Figure 1 schematically shows the structure of C/h-BN HBL in which (a) represents a typical structure, (b)-(d) represent top-down views of three different configurations.

## 3 Results and Discussions

Our calculated LDA lattice constants of graphene and h-BN mono-layer respectively turned out as  $a_0(\text{C}) = 2.445 \text{ \AA}$  and  $a_0(\text{BN}) = 2.488 \text{ \AA}$ , which are in excellent agreement with the reported values for graphene ( $a_0(\text{C}) = 2.445 \text{ \AA}$  in Ref. (11),  $2.4426 \text{ \AA}$  in Ref (17),  $2.4431 \text{ \AA}$  in Ref (37)) and mono layer h-BN ( $a_0(\text{BN}) = 2.488 \text{ \AA}$  in Ref. (16),  $2.4870 \text{ \AA}$  in Ref (37)) based on plane wave pseudo-potential method. Graphene turned out as gap-less, while mono-layer h-BN with its valence-band

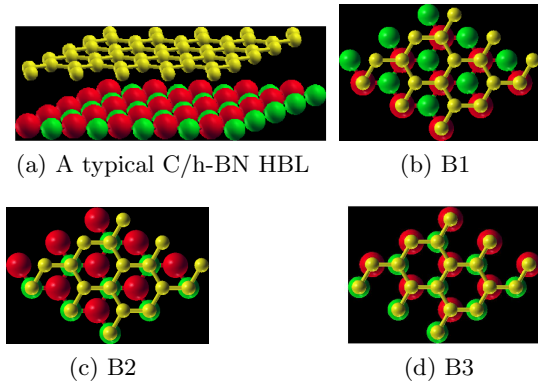


Figure 1: Ball-stick-model of C/h-BN HBL with top-down views of three different configurations B1, B2 and B3. (a) A typical structure; (b) B1, one C atom (small ball (yellow)) directly above the B atom (big ball (red)) and other C atom above the center of h-BN hexagon; (c) B2, similar to B1 with B replaced by N (medium ball (green)); (d) B3, one C atom is directly above the B and the other C atom directly above N. (For interpretation of the references to color in this figure legend, the reader is referred to the web version of this article.)

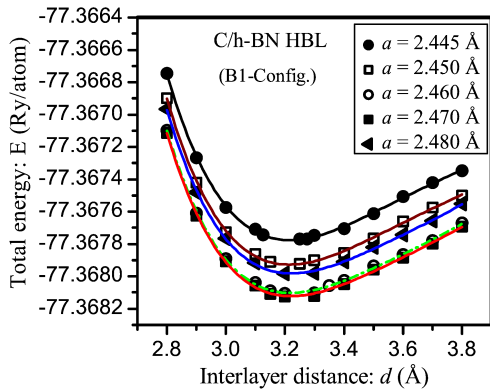


Figure 2: Total energy ( $E$ ) vs interlayer distance  $d$  at different  $a$  values of C/h-BN HBL(B1).

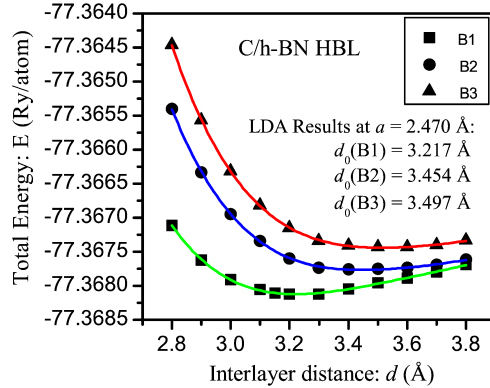


Figure 3: Variation of  $E$  with  $d$  at a common value of  $a = 2.47 \text{ \AA}$  for B1, B2 and B3 configurations of C/h-BN HBL.

maximum and the conduction band minimum located at K point of the Brillouin Zone (BZ), revealed a direct band gap of 4.606 eV, in agreement with previous calculations of 4.613 eV in Ref. [16], 4.35 eV in Ref. [37]. Our estimated band gap energy of h-BN mono-layer is about 23% less than the experimental [38] direct band gap energy of 5.971 eV.

The calculations for the composite structure of C/h-BN HBL were done as follows, unlike the earlier authors [11, 12] who used the LDA value of lattice constant of graphene ( $a_0(\text{C}) = 2.445 \text{ \AA}$ ) for the three configurations of C/h-BN HBL. As per the previous studies [11, 12], B1 configuration of C/h-BN HBL (henceforth we call it C/h-BN HBL(B1) or simply B1) is the most stable configuration with equilibrium interlayer spacing  $d_0(\text{B1}) = 3.22 \text{ \AA}$  at an assumed  $a_0(\text{B1}) = 2.445 \text{ \AA}$ . For B1, with which we are concerned in the present paper, the calculated ground state total energies at different  $d$  values for five fixed values of  $a$  ( $= 2.445, 2.450, 2.460, 2.470, 2.480 \text{ \AA}$ ) were obtained as depicted in Figure 2; from this

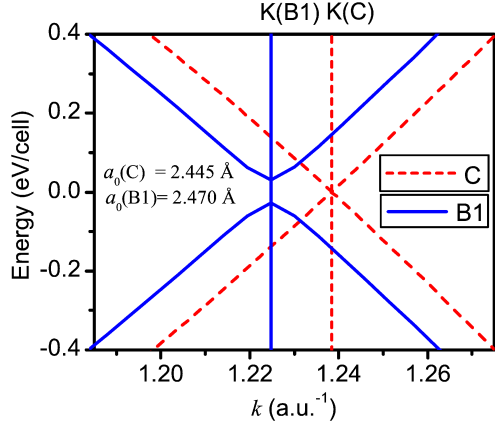


Figure 4: Comparison of energy bands (within LDA) of graphene (C) and C/h-BN HBL(B1) near the K point of the BZ. Fermi energy  $E_F = 0.0$  eV.

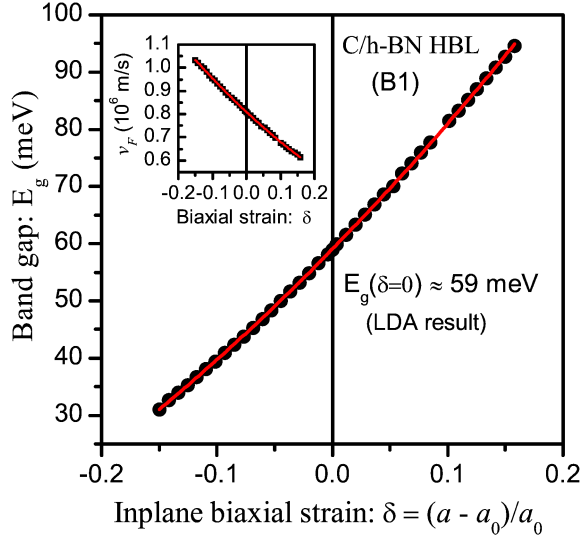


Figure 5: Variation of  $E_g$  of C/h-BN HBL(B1) with  $\delta$ . Inset shows the variation of Fermi velocity  $v_F$  with  $\delta$ .

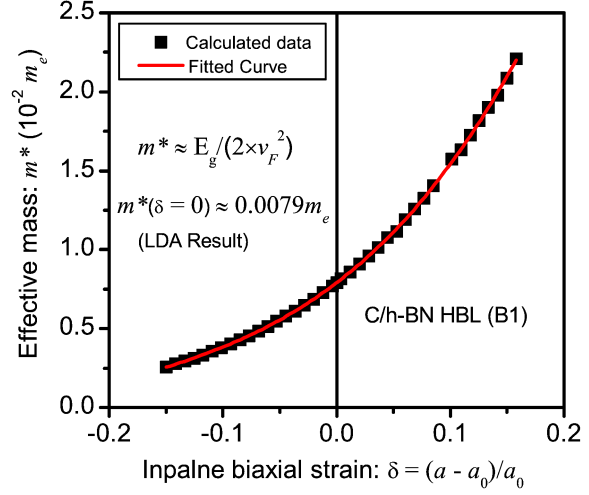


Figure 6: Variation of effective mass ( $m^*$ ) of charge carriers in C/h-BN HBL(B1) with  $\delta$ .

we estimated the optimized values of  $a$  and  $d$  as  $a_0(\text{B1}) = 2.47 \text{ \AA}$  and  $d_0(\text{B1}) = 3.217 \text{ \AA}$ . Similar calculations for B2 and B3 are required for a comparison of the relative stability of B1, B2 and B3. However, like previous authors [11, 12, 13], we got the relative stability and minimum interlayer distance of B1, B2 and B3 at constant  $a = 2.47 \text{ \AA}$  as depicted in Figure 3, which corroborate the reported results [11, 12, 13]. The interlayer spacing of B2 and B3 at a common value of  $a = 2.47 \text{ \AA}$  were estimated as  $d_0(\text{B2}) = 3.454 \text{ \AA}$ ,  $d_0(\text{B3}) = 3.497 \text{ \AA}$  which agree with the reported results [11, 12] of  $d_0(\text{B2}) = 3.4 \text{ \AA}$  and  $d_0(\text{B3}) = 3.5 \text{ \AA}$ .

The band structures of unstrained graphene and unstrained C/h-BN HBL(B1) near the K point of the BZ are depicted in Figure 4 for comparisons. As seen in Figure 4, graphene is gap-less, whereas C/h-BN HBL(B1) has a direct band gap of  $E_g = 59 \text{ meV}$  which is of same order of magnitude as that of graphene on a hexagonal BN substrate [11] ( $E_g = 53 \text{ meV}$ ) in

the same configuration. Therefore, the number of h-BN layers below graphene mono-layer has little impact on the band structure of C/h-BN heterostructure. It is to be noted that  $E_g$  is under-estimated here because of the LDA. However, in experiments [2] involving graphene on h-BN substrates, there is no evidence of this gap from transport measurements and this absence of gap has been attributed to randomly stacked graphene on h-BN [2]. The fabrication of a graphene/h-BN heterostructure with a desired alignment seems to be a technological hurdle at present. However, we note that Fan et al. [13] have investigated one type of misalignment of graphene to h-BN layer (along with the three aligned structures B1, B2 and B3 we have considered), which they have achieved by translating BN mono-layer a distance of  $\sqrt{3}a/6$  ( $a$  is the lattice constant of graphene) with respect to graphene along the C-C bond orientation from a pattern that corresponds to the B3 configuration of our present study. This misaligned heterostructure with an estimated equilibrium interlayer distance of 3.4 Å is energetically shown [13] to be unstable with respect to the most stable configuration that corresponds to the B1 configuration of our present study. Further, this misaligned structure is pictorially shown to have a small band gap which vanishes when the interlayer distance reaches 4.0 Å. It is to be noted that the theoretical study in [13] is concerned with the effect of interlayer spacings on electronic structure of graphene/h-BN hetero-bilayer and there is no consideration of biaxial strain effects. We also note that since our simulated homogeneous biaxial strain preserves the hexagonal symmetry of an aligned C/h-BN HBL (say B1), a misalignment is not expected to occur in such C/h-BN HBL under homogeneous biaxial strain which only affect the size but not the shape of the

hexagonal structure under study.

The energy dispersion around K point of BZ is linear for graphene and therefore the low energy quasi-particles mimic the massless Dirac fermion behavior[3, 4], i.e.,

$$E_{\pm} \simeq E_F \pm \hbar v_F k \quad (4)$$

where  $E_F$  is Fermi energy,  $v_F$  is Fermi velocity of quasi-particles, and  $(\hbar k)$  is the momentum. In case of B1, low energy dispersion is not only linear in  $k$  but also parallel to the low energy dispersion of graphene, while very low energy dispersion within an energy window of (-0.06 eV , +0.06 eV) around  $E_F$  ( $= 0.0$  eV) seems quadratic. Since the major portion of the energy dispersions around the K point (Dirac point) have identical slopes (hence identical  $v_F$  values) for graphene and C/h-BN HBL(B1), we attribute this to one of the reasons for B1 (in spite of having a small energy gap) behaving like free standing graphene as observed experimentally. From the linear energy dispersion portion of the plot, the calculated average value of  $v_F$  turned out as  $0.8 \times 10^6$  m/s for both graphene and C/h-BN HBL(B1), in agreement with other calculated result[13] and in close proximity of the experimental value  $\approx 10^6$  m/s for graphene [3, 4, 39]. Assuming that the effective mass ( $m^*$ ) of charge carriers of C/h-BN HBL at Dirac point given by the relation [13]  $m^* \simeq E_g/2v_F^2$ , we estimated  $m^* \simeq 0.0079m_e$  for B1 (where  $m_e$  is the free electron mass), which is much smaller than the effective Dirac fermions mass of  $0.03m_e$  in bilayer graphene [40]. The high value of  $v_F$  (equal to the  $v_F$  value in graphene), a very low value of  $m^*$  can render C/h-BN HBL pristine graphene-like electronic properties. However, it is to be noted that the observed pristine graphene-like electronic properties of C/h-BN HBL(B1) can not be attributed to these fac-

tors alone. This is due to the fact that experimentally the graphene/h-BN systems are fabricated by mechanical ex-foliation and transfer, so the stacking between graphene and BN can not be pre-determined and relaxed in such techniques.

For C/h-BN HBL(B1), the calculated variation of (i)  $E_g$  with in-plane homogeneous biaxial strain  $\delta = (a - a_0)/a_0$  is depicted in Figure 5, the inset shows the variation of  $v_F$  with  $\delta$ ; (ii)  $m^*$  with  $\delta$  is depicted in Figure 6.

Our predicted strain-induced modifications of  $E_g$ ,  $v_F$  and  $m^*$  should affect the transport and optical properties of C/h-BN HBL, which may be probed experimentally in a set-up (thought of as a specific amalgamation of the reported experimental [1, 2, 8] designs) like the one schematically shown in Figure 7. Although further improvements in the design and materials of Figure 7 are possible, the important message is that such an experiment is feasible with the available technology as applied successfully in the experiments [1, 2, 8]. In Figure 7, a simple h-BN back-gated BN-GFET[1, 2] is rigidly fixed on a variable biaxial strain inducing system (VSIS) like the one described in Ref. [8]. By applying a definite voltage across the VSIS, a biaxial strain of definite magnitude can be induced in BN-GFET. The current-voltage characteristics of the back-gated BN-GFET at different strain conditions may be studied to see to what extent the biaxial strain affects the transport properties of BN-GFET. Moreover, an optical probe of the direct band-gap of C/h-BN HBL may be performed at different strained states of BN-GFET in such a set-up. This opto-mechanical probe may ascertain if C/h-BN HBL can be used in designing nano opto-mechanical systems (NOMS).

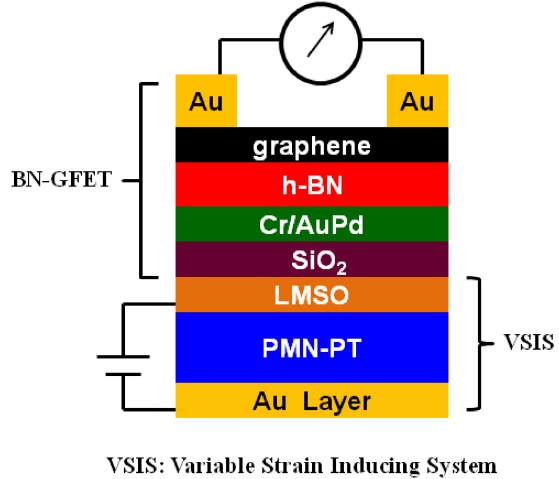


Figure 7: Schematic view of the proposed experimental set-up to study the strain-induced modifications of the electronic properties of C/h-BN HBL. Specific materials and fabrication schemes may be found in the experiments [1, 8].

## 4 Conclusions

In conclusion, we have studied and compared the band structures of graphene and C/h-BN HBL (in biaxially strained and unstrained states) using density functional theory based FP-(L)APW+lo method. From the parallel slopes of the energy dispersion bands near K point of the BZ of these structures, we estimated identical values of Fermi velocity of the low energy charge carriers in them. From this and an estimated small value of effective mass  $m^* \simeq 0.0079m_e$ , we infer the pristine graphene-like electronic properties of narrow-gapped C/h-BN HBL. However, these results do not necessarily reflect the measured transport properties of actual devices. In particular, the other important factors determining the actual device performance include the flatness of the substrate, surface phonon energy

and scattering, and the trap charges as in the oxide substrates. The strain-induced modifications of the energy band gap, Fermi velocity and effective mass of charge carriers in C/h-BN HBL in its most stable configuration was studied in detail with output of some testable results for which a schematic experimental set-up has been proposed. The results, if verified, may find applications in future graphene-based NEMS, NOMS and other nano-devices.

## References

- [1] I. Meric, C. Dean, A. Young, J. Hone, P. Kim, K.L. Shepard, Technical Digest International Electron Devices Meeting, IEDM, 2010, 23.2.1.
- [2] C.R. Dean, A.F. Young, I. Meric, C. Lee, L. Wang, S. Sorgenfrei, K. Watanabe, T. Taniguchi, P. Kim, K.L. Shepard, J. Hone, *Nat. Nanotechnol.* 5 (2010), 722.
- [3] A.K. Geim, *Science* 324 (2009) 1530.
- [4] A.H. Castro Neto, F. Guinea, N.M.R. Peres, K.S. Novoselov, A.K. Geim, *Rev. Mod. Phys.* 81 (2009) 109.
- [5] N.M.R. Peres, *Rev. Mod. Phys.* 82 (2010) 2673.
- [6] S.D. Sarma, E.H. Hwang, *Phys. Rev. B* 83 (2011)121405(R).
- [7] R.T. Weitz, A. Yacoby, *Nat. Nanotechnol.* 5 (2010) 699.
- [8] F. Ding, H. Ji, Y. Chen, A. Herklotz, K. Dörr, Y. Mei, A. Rastelli, O.G. Schmidt, *Nano Lett.* 10 (2010) 3453.
- [9] M. L. Lee, E.A. Fitzgerald, M.T. Bulsara, M.T. Currie, A. Lochtefeld, *J. Appl. Phys.* 97 (2005) 011101.
- [10] M. Chu, Y. Sun, U. Aghoram, S.E. Thompson, *Annu. Rev. Mater. Res.* 39 (2009) 293.
- [11] G. Giovannetti, P.A. Khomyakov, G. Brocks, P.J. Kelly, van den J. Brink, *Phys. Rev. B* 76 (2007) 073103.
- [12] J. Sławińska, I. Zasada, Z. Klusek, *Phys. Rev. B.* 81 (2010) 155433.
- [13] Y. Fan, M. Zhao, Z. Wang, X. Zhang, H. Zhang, *Appl. Phys. Lett.* 98 (2011) 083103.
- [14] J. Sławińska, I. Zasada, P. Kosiński, Z. Klusek, *Phys. Rev. B* 82 (2010) 085431.
- [15] A. Ramasubramaniam, D. Naveh, E. Towe, *Nano Lett.* 11 (2011) 1070.
- [16] J. Li, G. Gui, J. Zhong, *J. Appl. Phys.* 104 (2008) 094311.
- [17] R.M. Ribeiro, V.M. Pereira, N.M.R. Peres, P.R. Briddon, A.H. Castro Neto, *New J. Phys.* 11 (2010) 115002.
- [18] M. Farjam, H. Rafii-Tabar, *Phys. Rev. B* 80 (2009) 167401.
- [19] G. Gui, J. Li, J. Zhong, *Phys. Rev. B* 80 (2009) 167402.
- [20] Seon-M. Choi, Seung-H. Jhi, Young-W. Son, *Phys. Rev. B* 81 (2010) 081407(R).
- [21] Z.H. Ni, T. Yu, Y.H. Lu, Y.Y. Wang, Y.P. Feng, Z.X. Shen, *ACS Nano* 2 (2008) 2301.
- [22] T.M.G. Mohiuddin, A. Lombardo, R.R. Nair, A. Bonetti, G. Savini, R. Jalil,



- N. Bonini, D.M. Basko, C. Galiotis, N. Marzari, K.S. Novoselov, A.K. Geim, A.C. Ferrari, *Phys. Rev. B* 79 (2009) 205433.
- [23] M. Huang, H. Yan, T.F. Heinz, J. Hone, *Nano Lett.* 10 (2010) 4074.
- [24] O. Frank, M. Mohr, J. Maultzsch, C. Thomsen, I. Riaz, R. Jalil, K.S. Novoselov, G. Tsoukleri, J. Parthenios, K. Papagelis, L. Kavan, C. Galiotis, *ACS Nano* 5 (2011) 2231.
- [25] K.S. Kim, Y. Zhao, H. Jang, S.Y. Lee, J.M. Kim, K.S. Kim, Jong-H. Ahn, P. Kim, Jae-Y. Choi, B.H. Hong, *Nature* 457 (2009) 706.
- [26] E. Sjöstedt, L. Nordström, D.J. Singh, *Solid State Commun.* 114 (2000) 15.
- [27] E. Wimmer, H. Krakauer, M. Weinert, J.A. Freeman, *Phys. Rev. B* 24 (1981) 864.
- [28] Elk is an open source code: <http://elk.sourceforge.net/>
- [29] J.P. Perdew, A. Zunger, *Phys. Rev. B* 23 (1981) 5048.
- [30] H. Behera, G. Mukhopadhyay, *AIP Conf. Proc.* 1313 (2010) 152.
- [31] H.J. Monkhorst, J.D. Pack, *Phys. Rev. B* 13 (1976) 5188.
- [32] F. Liu, P. Ming, J. Li, *Phys. Rev. B* 76 (2007) 064120.
- [33] E. Cadelano, P. L. Palla, S. Giordano, L. Colombo, *Phys. Rev. Lett.* 102 (2009) 235502.
- [34] X. Wei, B. Fragneaud, C. A. Marianetti, J. W. Kysar, *Phys. Rev. B* 80 (2009) 205407.
- [35] C. Lee, X. Wei, J. W. Kysar, J. Hone, *Science* 321(5887) (2008) 385.
- [36] G. Cocco, E. Cadelano, L. Colombo, *Phys. Rev. B* 81 (2010) 241412.
- [37] S. Wang, *J. Phys. Soc. Jpn.* 79 (2010) 064602.
- [38] K. Watanabe, T. Taniguchi, H. Kanda, *Nat. Mater.* 3 (2004) 404.
- [39] K.S. Novoselov, A.K. Geim, S.V. Morozov, D. Jiang, M.I. Katsnelson, I.V. Grigorieva, S.V. Dubonos, A.A. Firsov, *Nature* 438 (2005) 197.
- [40] E.V. Castro, N.M.R. Peres, J.M.B.L. dos Santos, F. Guinea, A.H. Castro Neto, *J. Phys.: Conf. Ser.* 129 (2008) 012002.